*American Journal of Mechanical Engineering, 2017, Vol. 5, No. 2, 33-40*
Available online at http://pubs.sciepub.com/ajme/5/2/1

DOI:10.12691/ajme-5-2-1

# Fatigue Damage of Vertical Rigid Risers due to In-Line Vortex Induced Vibration in Nigeria Shallow Waters

**Tobechukwu C. Ezeonwumelu[1], Chinwuba V. Ossia[1,*], Ibiba E. Douglas[2]**

[1]Offshore Technology Institute, Faculty of Engineering University of Port Harcourt, Port Harcourt, Nigeria
[2]Marine Engineering Department, Rivers State University of Science & Technology, Port Harcourt, Nigeria
*Corresponding author: ossiacv@otiuniport.org

**Abstract** In-line and Transverse Vortex Induced Vibrations (VIV) pose potential Fatigue damage threat to Vertical Rigid Risers (VRR) even in the less volatile Nigeria Shallow Waters. In this paper, a typical VRR of 31.031m length clamped to a fixed jacket platform in 18.29m water depth was used while relevant metOcean data were used to simulate the environmental conditions. The process was statically and dynamically simulated using different wave spectra on Orcaflex platform. The results from JONSWAP spectra showed a fatigue damage value of 102.5 x $10^{-5}$ due to in-line VIV which is greater than 29.1 x $10^{-5}$ due to transverse VIV. The results from the Ochi-Hubble spectra indicate a fatigue damage value of 96.2 x $10^{-5}$ due to in-line VIV which is greater than 7.03 x $10^{-5}$ due to transverse VIV. Also, the in-line vortex force (VF) analysis on the VRR for the JONSWAP spectra showed VF range, beginning from the touchdown point (TDP) to the unstraked region (UR), of 0.16 - 0.34kN/m; 0.01 - 0.53kN/m; and 0 - 0.85kN/m at End A (0m); 8.74m and 21.00m, respectively. Whereas, for the Ochi-Hubble spectra, VF range, from TDP to the UR, of 0.16 - 0.302kN/m; 0.018 - 0.56kN/m; 0 - 1.42kN/m at End A (0m); 8.74m and 21.00m, respectively, were obtained. The results for both spectra showed zero in-line VF on the VRR at 23.69m, 26.21m and End B (31.031m). Hence, fatigue damage and VF due to in-line VIV is important from the TDP to most parts of the UR on the VRR irrespective of the wave spectra and requires proper analysis in riser designs.

***Keywords:*** *in-line vortex induced vibration, transverse vortex induced vibration, fatigue damage value, vertical rigid risers, Nigeria shallow waters*

**Cite This Article:** Tobechukwu C. Ezeonwumelu, Chinwuba V. Ossia, and Ibiba E. Douglas, "Fatigue Damage of Vertical Rigid Risers due to In-Line Vortex Induced Vibration in Nigeria Shallow Waters." *American Journal of Mechanical Engineering*, vol. 5, no. 2 (2017): 33-40. doi: 10.12691/ajme-5-2-1.

## 1. Introduction

Marine risers are exposed to several environmental conditions which include wave, current, tides, wind, etc. When exposed to current, a stationary circular cylinder such as a rigid riser experiences flow around it and this flow is characterized by large zones of separation which causes the riser to build-up a surrounding boundary layer due to skin friction between the fluid and the body. Leonardo Da Vinci in 1497 was probably the first to pay attention to how flow separates from the surface of different objects and what types of pattern were formed in their wakes [1]. In 1883, Reynolds in investigating internal flow in pipes discovered that the transition between laminar and turbulence was a function of the density, viscosity and velocity of the fluid and of the diameter of the pipe [1]. Reynolds number (Re) tells us whether a flow is laminar or turbulent, and expresses the relationship between inertia and viscous forces in a flow.

Marcollo [2] deduced that at certain critical values, the flow transits from laminar to turbulence in which disturbances from other effects can affect this Re-value. Such effects might be roughness, turbulence and any cylinder oscillations as suggested by Zdravkovich [3]. Reynolds determined that the transition to turbulence happened within a range of Re. Reynolds number (Re) governs the effect of flow around circular cylinders which includes the transition states. Transition in the shear layer was discovered as Re was rising, the transition zone moved towards the separation points changing the length and width of the near wake region [4].

Also, Huera-Huarte [1] stated that there is an adverse pressure gradient in the direction of the flow which causes the boundary layer to separate from the surface of the cylinder generating a recirculation in the flow. The result of this phenomenon is the wake being formed around it. The result of the mutual interaction between two separating shear layers is the fundamentals of vortex shedding as emphasized by Gerrard [5]. Vortex shedding is the result of an interaction between the shear layers in the near body wake involving the inherent vorticity [1], but according to Marcollo [2], the phenomenon is an instability intrinsic to the flow itself. As further explained by Sarkpaya [6], it is a consequence of the interaction between shear layers, base pressure, diffusion and dissipation of vorticity. Separation begins at Re = 4, this continues until the Re = 47 where the near wake is observed to be unstable leading to vibrations of the shear layer at the neutral point. There is a common feature for circular cylinder flows with Re > 47, that is vortex

shedding and the formation of the Karman-Bernard vortex street [1]; hence flow instability produces vortices that grow alternately on each side of the body [5]. At about Re = 47, the vortex shedding frequency or Strouhal frequency appears. For smooth cylinderical surfaces, Strouhal number $S_t$ is found to be nearly constant at 0.2 to 0.25 for $5x10^2 < Re < 2x10^5$. HueraHuarte [1] showed, from experiments carried out by different researchers, that the frequency of the vortex shedding in the wake of a cylinder is a function of Re, the roughness of the cylinder surface, the turbulence intensity in the incoming flow, the aspect ratio, the blockage ratio, etc. The Strouhal number ($S_t$) is a function of the roughness and the incoming turbulence. The roughness on a cylinder has effect on the $S_t$ with the largest effect being in the critical Re region [2]. Furtherrmore, Achenbach and Heinecke [7] suggested that the greater the roughness, the lower the $S_t$ – value in the critical region, likewise for a smooth cylinder, the $S_t$ is seen to more than double in this region.

These motions generated from the effects of vortices are known as Vortex Induced Vibrations (VIV). VIV phenomenon plays a significant role in marine riser analyses with respect to fatigue. In general, VIV is viewed in two aspects namely; the cross-flow VIV and in-line VIV which is due to lift and drag forces, respectively. In-line VIV is due to drag forces acting in the direction of flow. The drag is a measure of the resistance offered to flow by a body. Traditionally, focus has been on cross-flow VIV [8]. In-line VIV was considered less important because the displacements were smaller but Baarholm et al. [9] found that the fatigue damage due to in-line VIV can be equally important. This is mainly because in-line forces occur at twice the frequency of the cross-flow forces, causing the structure to vibrate in higher modes [8].

Aronsen [10] carried out experimental investigations between in-line and cross flow VIVs. Experiments were performed in a towing tank of 40m using a rigid cylinder of aspect ratio 20 under prescribed harmonic motions in uniform flow. The cylinder was installed in a yoke structure which in turn was suspended to an overhanging tow carriage. Model oscillations were achieved by oscillating the yoke on the carriage while the flow velocity was obtained by moving the carriage at constant speed in still water. All the experiments were performed at a Re = $2.4 \times 10^4$. The aim was to investigate hydrodynamic coefficients for pure in-line oscillations as well as the interactions between in-line and cross flow VIV. From the first experiment on in-line oscillations, where the frequencies and amplitude were varied to obtain a detailed map of the forces acting on a cylinder in the pure in-line VIV regime, it was discovered that in-line oscillations will give rise to cross-flow forces that contribute to an early start-up of VIV, compared to conditions where the in-line motion is restrained.

Also, based on experiments carried out on a riser in Hanoytangen - Norway, Baarholm et al. [9] discovered that low current velocities tend to activate tension controlled modes (low order modes) which eventually cause fatigue due to In-line VIV. Similarly, the lowest modes (that is, from low current speeds), has significant contribution to fatigue damage because at this condition, in-line oscillations occur at double the frequency for the cross-flow. It was also discovered that In-line fatigue damage is due to a combination of water depth and current velocity (that is, fatigue due to in-line VIV will increase for a decreasing velocity and an increasing water depth). Also in-line fatigue damage was found to be significant at the bottom of the riser where current speeds are low. It can be shown that the fatigue damage is proportional to $U^7$ (flow velocity) and $U^4$ when the response is dominated by tension and bending stiffness controlled modes, respectively. The Hanoytangen riser fatigue damage was proportional to $U^7$ for the lowest velocities. It was also observed that the tension controlled case, corresponds to a mode with half the wavelength and since the curvature for the amplitude increases with mode wavelength squared; fatigue for in-line VIV tends to dominate for cases with tension controlled modes.

Thorsen et al. [8] showed that a number of models are available for predicting VIVs which include; computational fluid dynamics, wake oscillator models and semi-empirical models. Wake oscillator models use a Van de Pol oscillator to describe the fluid force in the time domain [11]. Ge et al. [12], presented a wake oscillator model for combined in-line and cross-flow VIV of a tensioned beam. While semi-empirical models such as VIVANA use coefficients from forced vibrations and apply iterative procedures to calculate the frequency, mode and amplitude of vibration [13]. Semi-empirical and wake oscillator models were originally able to calculate cross flow VIVs only, while some of the models have also been extended to include in-line VIV as indicated by Chaplin et al. [14]. Recently, Thorsen et al. [8], in their work, a time domain simulation method for a combined cross-flow and in-line VIV was presented. The key results were compared to experimental observations with an observation that the predicted curve was very realistic for the in-line direction, while slightly conservative for the cross-flow direction.

The time domain simulation process takes into consideration the wave effects in marine riser analyses; hence the inclusion of the JONSWAP and Ochi-Hubble wave spectra as comparative case studies in this work. Hasselmann et al. [15], showed that a JONSWAP spectra was developed where a peak enhancement factor was included as a modification to the Pierson-Moskowitz spectra as shown in Equation 1;

$$S(f) = \propto g^2 (2\pi)^{-4} f^{-5} e^{\left(-1.25\left(\frac{f_p}{f}\right)^4\right)} * \gamma^{\exp\left\{\frac{(-f-f_p)^2}{2\sigma^2 f_p{}^2}\right\}} \quad (1)$$

Where $\sigma = \sigma_a$ for $f < f_p$ and $\sigma = \sigma_b$ for $f > f_p$, $f_p$ represents the spectral peak frequency.

The JONSWAP spectrum contains 5 parameters $f_p$, $\alpha$, $\gamma$, $\sigma_a$ and $\sigma_b$ and the most probable values for some of these read: $\gamma$=3.3, $\sigma_a$= 0.07 and $\sigma_b$=0.09 .The values for $\alpha$ and $f_p$ depend on the wind speed, fetch and duration.

Similarly, Ochi and Hubble [16] formulated the double peak spectra model shown in Equation 2;

$$S(f) = \sum_{j=1}^{2} \frac{H_{sj}{}^2 T_{pj} (\lambda_j + 0.25)^{\lambda_j}}{4\Gamma(\lambda_j)(T_{pj} f)^{(4\lambda_j+1)}} \exp\left[-\frac{(\lambda_j + 0.25)}{(T_{pj} f)^4}\right] \quad (2)$$

Where $\Gamma$ is the gamma function.

This spectrum has 3 parameters for each wave system, significant wave height ($H_{sj}$), spectral peak period ($T_{pj}$) and the shape factor ($\lambda_j$).

In summary, relevant available literature show that initial focus was on the cross-flow VIV until the significance of in-line VIV was brought to limelight only recently [8,9], and [10]. Aronsen [10] carried out experiments in Norway to determine certain in-line oscillation parameters, while Baarholm et al. [9] compared his computer program results on fatigue damage to an existing experimental data measured in Norway. Thorsen et al. [8] then presented a time domain method for simulating both cross-flow and in-line VIVs. From the reviews it can be shown that there is insufficient experimental work and time domain simulations of in-line VIV in the tropical regions well impacted by the phenomenon. International Oil Companies are always on course in maximally applying best operational practices that maximize profit and minimize cost over a long period of time. In-line VIV is an anathema to the long time performance of VRRs in shallow waters. With major offshore projects to take place in West Africa, it becomes necessary to undertake adequate research on this phenomenon simulating this particular environment to ensure proper design of VRRs in this region at minimal costs. In-line VIV is important in low current offshore environments with shallow water depths as well as tensioned steel risers; hence, the reason for research into vertical rigid risers (VRR) for a fixed jacket platform in Nigeria shallow waters. This study therefore shows results from simulating a typical VRR for a shallow water Offshore platform using metOcean data of the region with JONSWAP and Ochi-Hubble wave spectra on OrcaFlex 8.47a [17] platform with a view to analyzing the VIV effects on fatigue damage.

## 2. Materials and Methods

### 2.1. Riser Material Properties

Data on a typical VRR for a fixed jacket platform in Nigeria Shallow water were collated. The relevant rigid Riser material properties include: Seamless Carbon Steel, Outer diameter (OD) $\phi$12.75 inch, inner diameter (ID) $\phi$11.278 inch, wall thickness (WT) 0.736 inch, and Specified minimum yield strength (SMYS) of 448MPa. These material data were imputed into the OrcaFlex platform. Figure 1, Figure 2 and Figure 3 are snapshots from the OrcaFlex platform showing relevant data imputed.

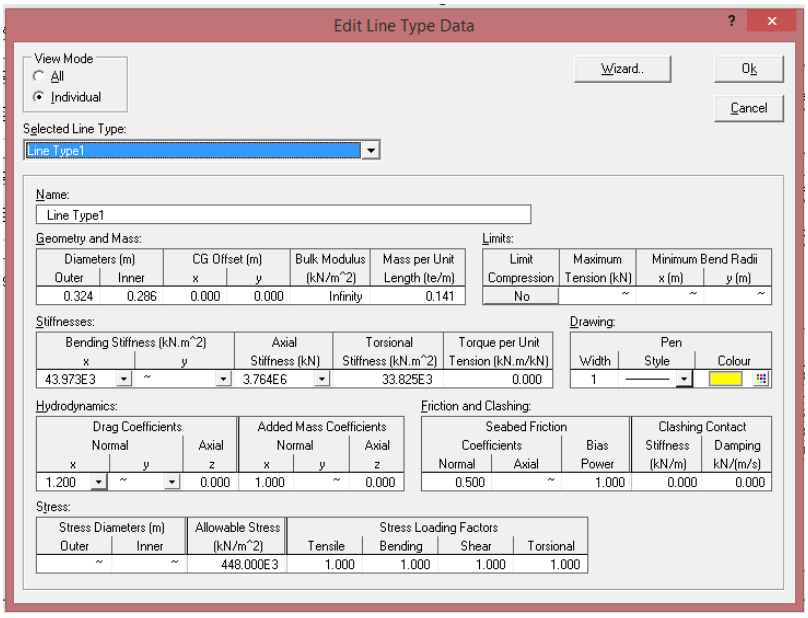


**Figure 1.** VRR Material Description on OrcaFlex Interface 1

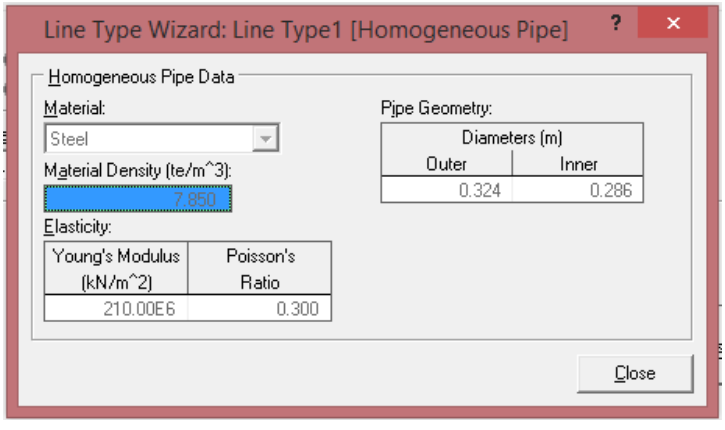


**Figure 2.** VRR Material Description on OrcaFlex Interface 2

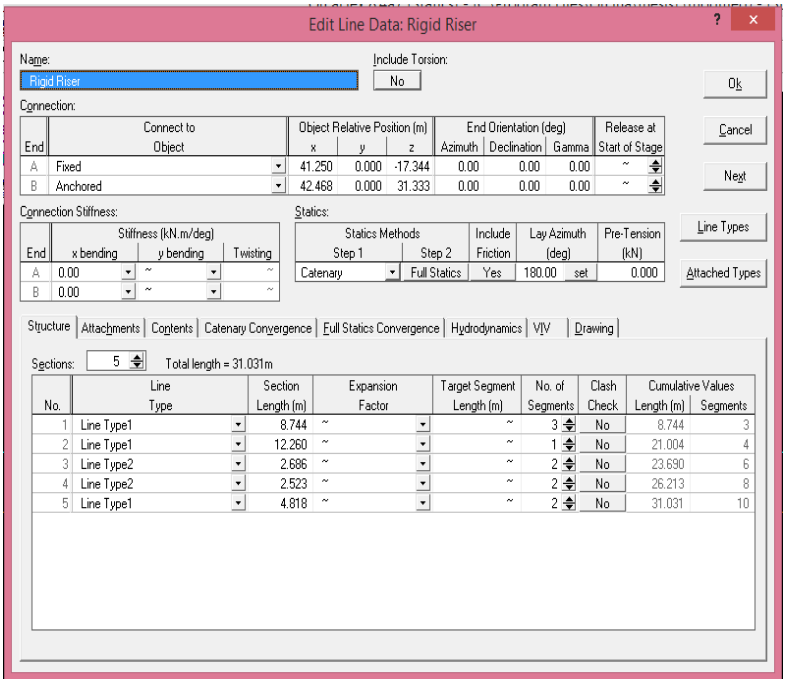


**Figure 3.** VRR Material Description on OrcaFlex Interface 3

## 2.2. MetOcean Data

MetOcean data showing water depth, current factor, rotation, near- surfaces and near-bottom current speed and direction for Offshore Nigeria Waters were obtained and shown in Figure 4 and Figure 5.

Another metOcean data involving the near-bottom surface current velocity versus simulation time variation showed 0, 0.103, 0.206, 0.309, 0.412, and 0.514m/s velocity for 0, 2, 4, 6, 8, and 10s simulation time, respectively.

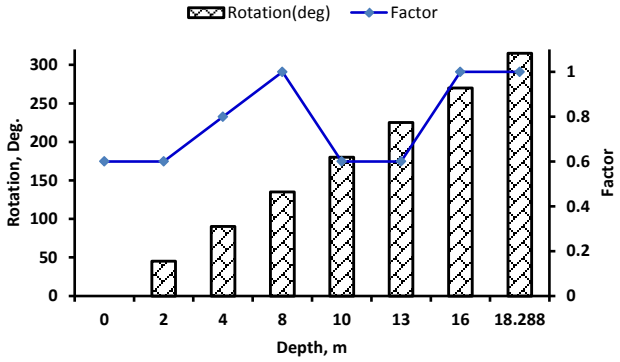


**Figure 4.** Current Factor and Angle of rotation for various water depths

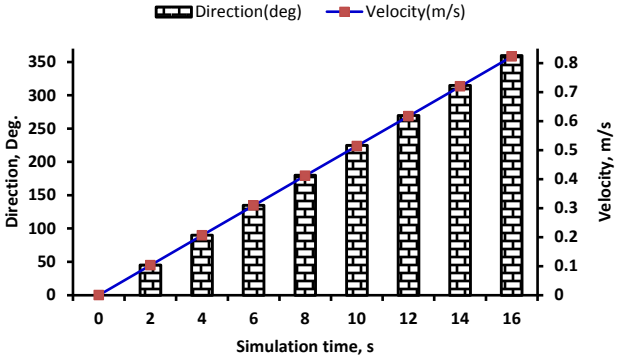


**Figure 5.** Near Surface Current velocity and Direction versus simulation time

## 2.3. Methods

Firstly, the data for the riser material and metOcean characteristics were inputted on the Orcaflex8.4a7 [17] Software, and simulated with using the Milan wake oscillator model. Results were obtained for the In-line (drag) and Transverse (lift) vortex forces. These two vortex forces scenarios were adequately subjected to fatigue analysis with interest on In-line VIV Analysis while the Transverse VIV Analysis was used for comparison. The fatigue damage values were therefore obtained and analyzed.

# 3. Results and Discussion

## 3.1. JONSWAP Wave Spectra

### 3.1.1. Fatigue Damage Analysis

Raw data from Figure 4, Figure 5 and the other metOcean data involving the near-bottom surface current velocity versus simulation time variation were inputted into the environment and variable data section of the OrcaFlex platform.

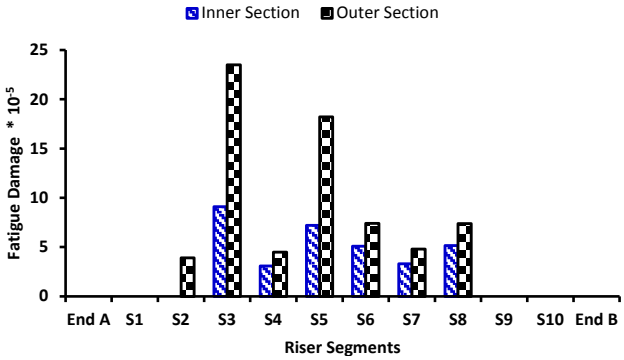


**Figure 6.** Variation of Fatigue damage due to In-line VIV with Riser segments

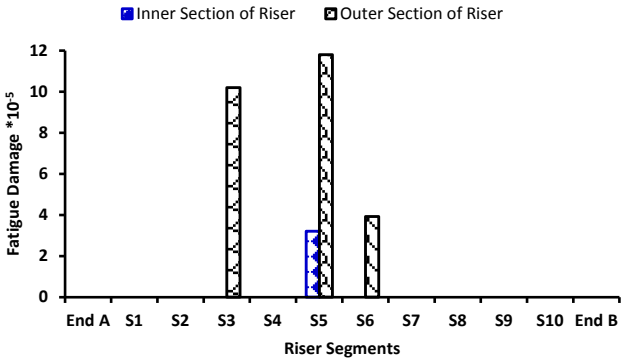


**Figure 7.** Variation of Fatigue Damage due to Transverse VIV with Riser segments

The results from Figure 6 show a fatigue damage due to in-line vortex induced vibration for both the inner and outer section of the 31.031m riser length from End A, Segments 1 to 10, up to End B. End A, Segments 1, 9, 10 and End B showed no damage at all while Segment 2 recorded damage only at the outer section of the riser. Segments 2 to 8 (from about 4.372m to 25.582m) recorded damage for both inner and outer sections with damage due to the outer sections greater than the corresponding inner sections. These results indicate that at TDP, some parts of the unstraked region and hang-off section of the riser, fatigue damage is not important. Total Fatigue damage for the inner section is 32.9 x $10^{-5}$ and 69.6 x $10^{-5}$ for the inner and outer section of the riser, respectively; giving a total fatigue damage of 102.5 x $10^{-5}$ on the riser.

The results from Figure 7 show fatigue damage due to transverse vortex induced vibration for both the inner and outer section of the riser for End A, Segments 1 to 10, up to End B. No fatigue damage value was observed for End A, Segment 1, 2, 4, 7, 8, 9, 10 and End B while Segments 3, 5 and 6 showed responses with no value for the inner section at Segment 3 and 6. These results indicate that at the touchdown point, hang-off region and most part of the unstraked region, fatigue damage is not important. Total Fatigue damage due to transverse VIV for the inner section is 3.2 x $10^{-5}$ and 25.9 x $10^{-5}$ for the inner and outer section of the riser, respectively; giving a total fatigue damage of 29.1 x $10^{-5}$ on the riser. Figure 6, and Figure 7 clearly show that transverse VIV is not relevant in the design of VRRs for shallow waters application in the Gulf of Guinea, since the fatigue damage is zero / insignificant. Also, comparing the total fatigue damage values of both the In-Line and Transverse analysis shows that of In-Line to be greater, hence less fatigue life. This implies that in design applications for VRR in this region, In-line VIV should be considered a priority.

### 3.1.2. Vortex Force Analysis

Vortex forces (VF) results for the VRR hang-off region - "End A" in Figure 8 showed maxima at (t, VF) = (2.2, 0.165); (6.7, 0.34); (13.4, 0.33) and minima at (t, VF) = (0.98, 0.16); (3.1, 0.16) (10.0, 0.16). The node, "End A" on the riser lies on the seabed or mudline and was subjected near-bottom currents with low velocities within the range of 0 – 0.514m/s. The impact of current at this node is quite minimal, regular and stable hence the reason for the resulting graph showing mesokurtic peaks with flat sags.

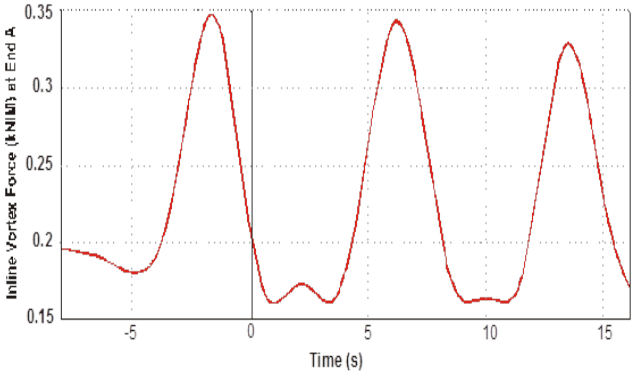


**Figure 8.** In-Line Vortex Force End A (0m) VRR

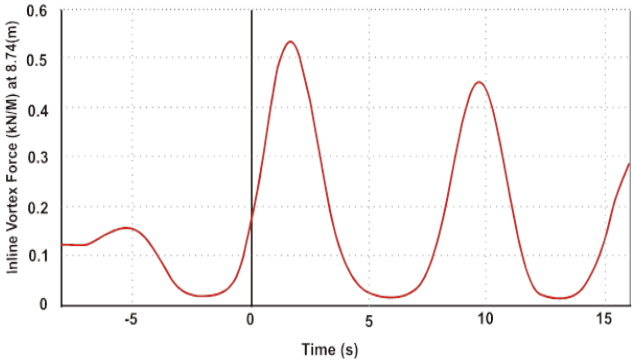


**Figure 9.** In-Line Vortex Force at 8.74m VRR

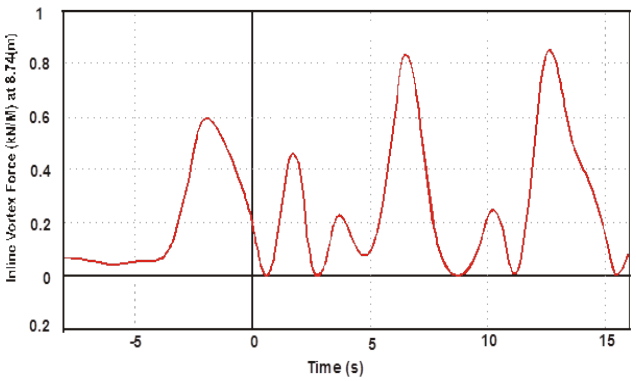


**Figure 10.** In-Line Vortex Force at 21.00m VRR

At the VRR segment 8.74m the VF results in Figure 9 showed maxima at (t, VF) = (1.8, 0.53); (9.8, 0.45) and minima at (t, VF) = (5.9, 0.01); (12.5, 0.01). This node, "8.74m" on the riser is within the submerged region. The currents impacting on this node are still low but slightly higher than that of End A. The current impact on the riser is a bit stable and regular hence the mesokurtic peaks with flat sags. Also the maxima VF acting on the riser tends to decrease as time increases over the simulation period.

For the 21.00m VRR vortex force results in Figure 10, maxima were observed at (t, VF) = (1.8, 0.45); (3.7, 0.23); (6.6, 0.83); (10.2, 0.24); (12.5, 0.85) and minima at (t, VF) = (0.6, 0); (2.8, 0); (4.9, 0.085); (8.8, 0); (11.2, 0); (15.4, 0). This node, "21.00m" on the riser is subjected to near-surface current velocities within the range of 0 – 0.823m/s and it is within the splash zone. At this zone, the riser node experiences surges of irregular current at different time intervals leading to continuous fluctuations of the VF and mesokurtic peaks with sharp gullies as shown on the graph. Also, the current velocity acting on this node is

higher as compared to that acting on the bottom surfaces. Hence, the reason for this node experiencing the highest maxima VF of 0.85kN/m as compared to nodes End A and 8.74m. Also, the in-line vortex force value at the maxima of the highest mesokurtic peak increased steadily from Figure 8 to Figure 10. This shows steady increase at the maximum as we go up from End A to node 21.00m.

Figure 11 shows zero vortex force throughout the simulation time on the riser, same as the situation at 26.21m and End B (31.031m). This is expected since this area connotes the atmospheric region around the VRR.

## 3.2. Ochi-Hubble Wave Spectra

### 3.2.1. Fatigue Damage Analysis

Raw data from Figure 4, Figure 5 and the other metOcean data involving the Near-bottom surface current velocity versus simulation time variation were inputted into the environment and variable data section of the OrcaFlex platform.

The results from Figure 12 show a fatigue damage values due to in-line vortex induced vibration for both the inner and outer section of the 31.031m riser for End A, Segments 1 to 10, up to End B. End A, Segments 1, 2, 8, 9, 10 and End B showed no damage at all while Segments 3 to 7 recorded damage between 7.287m to 24.321m of the entire riser section with Segment 7 indicating damage only at the outer section of the riser. From the results, fatigue damage at the touchdown point, some parts of the unstraked region and hang-off section of the riser is not important. Total Fatigue damage is 30.7 x $10^{-5}$ and 65.5 x $10^{-5}$ for the inner and outer section of the riser, respectively; giving a total fatigue damage of 96.2 x $10^{-5}$ on the riser.

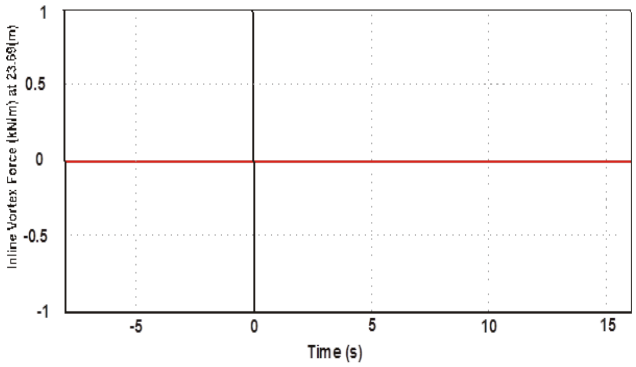


**Figure 11.** In-Line Vortex Force at 23.69m VRR

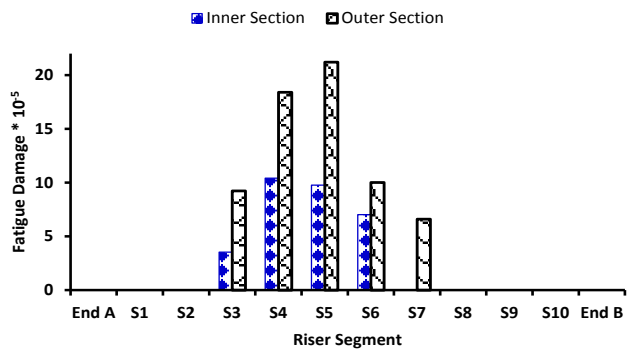


**Figure 12.** Variation of Fatigue Damage due to In-Line VIV with Riser segments


**Figure 13.** Variation of Fatigue Damage due to Transverse VIV with Riser segments

The results from Figure 13 show fatigue damage due to transverse vortex induced vibration for both the inner and outer section of the riser for End A, Segments 1 to 10, up to End B. No fatigue damage value was observed throughout the inner section of the riser while the outer section recorded values at Segment 4 and 5. These results indicate that at the hang-off region, touchdown point and most part of the unstraked region, fatigue damage is not important.

Total Fatigue damage due to transverse VIV for the inner section is zero and 7.03 x $10^{-5}$ for the inner and outer section of the riser, respectively; giving a total fatigue damage of 7.03 x $10^{-5}$ on the riser. Figure 12 and Figure 13 clearly show that transverse VIV is not relevant in the design of VRRs for shallow waters application in the Gulf of Guinea, since the fatigue damage is zero / insignificant. Also, comparing the total fatigue damage values of both the In-Line and Transverse analyses shows the In-Line case to be greater, hence less fatigue life. This implies that in design application for VRR in this region, In-line VIV should be considered a priority.

The Fatigue damage along the length of the Riser for both JONSWAP and OCHI – HUBBLE Spectra show similar trend: In both cases the In-Line Fatigue Damage rates are higher than those of the Transverse (that is, Cross flow) at all segments of the Riser. This is consistent with experimental results presented by Gedikli [18] which show the natural frequencies of the In-line Vibrations higher than the Cross Flow frequencies. This trend however also depends on flow Reynolds Number. Measured Cross Flow and In-Line fatigue damage rates associated with four different flow regimes obtained by Shi [19] also indicate that Fatigue Damage rates vary along the length of the Riser in a similar way hence supporting the results of the OrcaFlex Software analysis in this work. Also, results obtained using OrcaFlex showing steel catenary risers (SCR) fatigue life and tension variation with arc length have been reported by Chibueze et. al. [20].

### 3.2.2. Vortex Force (VF) Analysis

From Figure 14, the Vortex Force – time graph of End A (hang-off) showed maxima at (t, VF) = (4.4, 0.225); (8.8, 0.302); (12.6, 0.167); and minima at (t, VF) = (6.4, 0.18); (12, 0.16); (13.8, 0.162).

The node, “End A” on the riser lies on the seabed or mudline and was subjected near-bottom currents with low velocities within the range of 0 – 0.514m/s. The impact of

current at this node is quite minimal, regular and stable hence the reason for the resulting graph showing mesokurtotic peaks with flat sags.

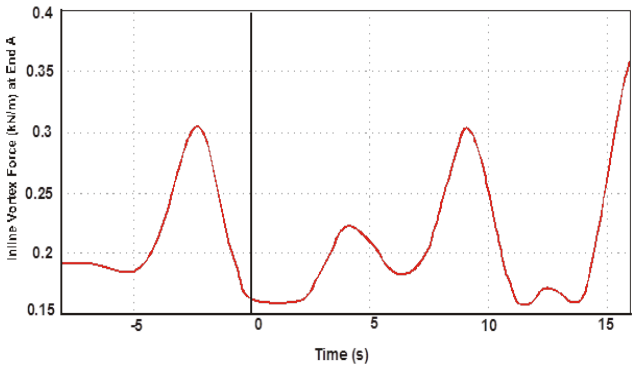


**Figure 14.** In-Line Vortex Force at End A (0m) VRR

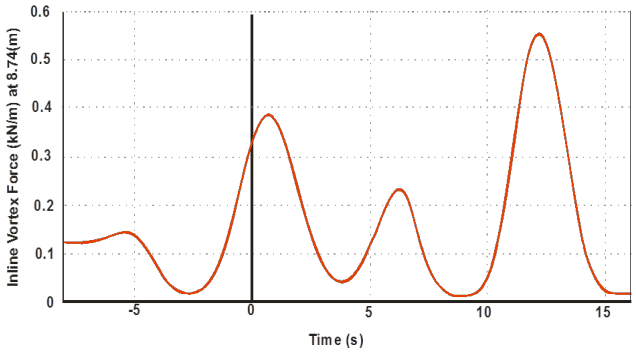


**Figure 15.** In-Line Vortex Force at 8.74m VRR

At VRR length 8.74m the vortex force – time plot showed maxima at (t, VF) = (1, 0.38); (6.2, 0.23); (12.2, 0.56); and minima at (t, VF) = (4.1, 0.045); (9.1, 0.018); (15, 0.021) as in Figure 15. This node, "8.74m" on the riser is within the submerged region. The currents impacting on this node are still low but slightly higher than that of End A. The current impact on the riser is a bit stable and regular hence graph showing mesokurtic peaks with flat sags. The VF tends to fluctuate with time over the simulation period.

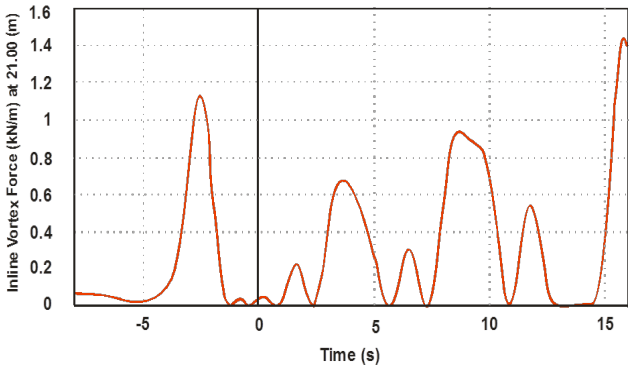


**Figure 16.** In-Line Vortex Force at 21.00m VRR

The Vortex force - time variant plot at VRR length of 21.00m in Figure 16 showed maxima at (t, VF) = (0.3, 0.04); (1.9, 0.22); (3.8, 0.69); (6.2, 0.32); (8.4, 0.94); (12, 0.54); (15.8, 1.42) and minima at (t, VF) = (1, 0); (2.4, 0); (5.8, 0); (7.3, 0); (11.1, 0); (13.7, 0). This node, "21.00m" on the riser is subjected to near-surface current velocities within the range of 0 – 0.823m/s and it is within the splash zone. At this zone, the riser node experiences surges of irregular current at different time intervals leading to the continuous fluctuations of the VF and mesokurtic peaks with sharp gullies as shown on the graph. Also, the current velocity acting on this node is higher as compared to that acting on the bottom surfaces. Hence, the reason for this node experiencing the highest maximum VF of 1.42kN/m as compared to nodes End A and 8.74m. Also, the in-line vortex force value at the maxima of the highest mesorkurtic peak increased steadily from Figure 14 to Figure 16. This shows steady increase at the maximum as we go up from End A to node 21.00m.

Similar to the results obtained for the JONSWAP spectra in Figure 11, the Ochi-Hubble spectra showed zero vortex force throughout the simulation time, same as the situation at 26.21m and End B (31.031m). This is expected since this area connotes the atmospheric region around the VRR.

## 4. Conclusion

The fatigue analysis due to In-line VIV based on the JONSWAP and Ochi-Hubble wave spectra for the VRR led to fatigue damage values of 102.5 x $10^{-5}$ and 96.2 x $10^{-5}$ which is greater than the fatigue damage value due to Transverse VIV of 29.1 x $10^{-5}$ and 7.03 x $10^{-5}$ for both spectra, respectively. It was also observed that on the 31.031m riser length, fatigue damage due to In-line VIV based on the JONSWAP spectra covered a wider span from 4.372m to 25.582m as compared to that based on the Ochi-Hubble spectra of span 7.287m to 24.321m. Also from the In-line Vortex force analysis on the VRR for both wave spectra, it can be seen that In-line Vortex Force is important from the touchdown point up till some point above the riser mid-point (that is, End A (0m) to 21.00m); but it is not important at most part of the unstraked region (UR) above the sea level up till the hang-off (that is, 21.01m to End B (31.031m)).

From the foregoing, it can be inferred that in Nigeria Shallow waters, In-line VIV is of priority in VRR fatigue failure design and analysis. Designing VRR based on the Ochi-Hubble wave spectra will decrease fatigue damage and hence increase fatigue life, unlike the JONSWAP spectra.

## Nomenclature

| | |
|---|---|
| VIV | - Vortex Induced Vibration |
| JONSWAP | - Joint North Sea Wave Project |
| U | - Flow Velocity |
| ID | - Inner Diameter |
| OD | - Outer Diameter |
| SMYS | - Specified Minimum Yield Strength |
| WT | - Wall Thickness |
| VF | - Vortex Force |
| Re | - Reynolds Number |
| St | - Strouhal Number |
| $H_s$ | - Significant wave height [m] |
| $T_s$ | - Average zero up-crossing period [s] |
| j | - Integer counter |
| $S_n$ | - wave spectral density [$m^2$/Hz] |
| $f_p$ | - Peak frequency [Hz] |

t - Time [s]
γ - Peakedness parameter (1 to 7)
α - Parameter
λ - Ochi-Hubble shape parameter (5 & 6)

# References


[1] Huera-Huarte, F.J. (2006). Multi-Mode Vortex-Induced Vibrations of a Flexible Circular Cylinder, A Doctoral thesis submitted in fulfilment of the requirements for the degree of Doctor of Philosophy to the Imperial College London, (University of London), pp. 24-35., January 2006.

[2] Marcollo H. (2002). Multimodal Vortex-Induced Vibration, A Doctoral thesis submitted in fulfilment of the requirements for the degree of Doctor of Philosophy to Department of Mechanical Engineering, Monash University, Victoria, Australia, 2002.

[3] Zdravkovich, M.M. (1997). Flow Around Cylindrical Structures. Vol 1: Fundamental (1st Edition). Oxford University Press

[4] Bloor, M..S. (1964). The Transition to Turbulence in the Wake of a Circular Cylinder. Journal of Fluid Mechanics, Vol. 19, pp. 290.

[5] Gerrard, J.H. (1996). The Mechanics of the Formation Region of Vortices behind Bluff Bodies; Journal of Fluid Mechanics, Vol. 25 (02), pp. 401-413.

[6] Sarkpaya, T. (1979). Vortex Induced Oscillations - A Selective Review. Journal of Applied Mechanics. Vol. 46, pp. 241-258.

[7] Achenbach, E. and Heinecke, E. (1981). On Vortex Shedding from Smooth and Rough Cylinders in the Range of Reynolds Numbers $6x10^3$ to $5x10^6$; Journal of Fluid Mechanics, Vol 109, PP.239-251.

[8] Thorsen, M.J., Saevik, S., Larsen C.M. (2014). Time domain simulation of cross-flow and in-line vortex induced vibrations; Proceedings of the 9th International Conference on Structural Dynamics, EURODYN, Porto, Portugal, 2014

[9] Baarholm, G.S., Larsen, C.M., Lie, H. (2006). On Fatigue Damage Accumulation from In-line and Cross-flow Vortex Induced Vibrations on risers. Journal of Fluids and Structures, Vol. 22 (01), pp.109-127.

[10] Aronsen, K.H. (2007). An Experimental Investigation of In-line and Combined In-line and Cross-flow Vortex Induced Vibrations; A Doctoral thesis submitted in fulfilment of the requirements for the degree of Doctor of Philosophy to Department of Marine Technology, Norges Teknis-Naturvitenkapelige Universitet, Trondheim, Norway, 1503-8181, 2007: 253.

[11] Facchinetti, M.L., de Langre, E., Biolley, F. (2004). Coupling of Structure and Wake Oscillators in Vortex Induced Vibrations. Journal of Fluids and Structures. Vol.19, pp. 123-140.

[12] Ge, F., Long, X., Wang, L., Hong, Y. (2009). Flow–Induced Vibrations of Long Circular Cylinders Modeled by Coupled Non Linear Oscillators. Science in China Series G: Physics, Mechanics and Astronomy, Vol. 52 (07), pp. 1086-1093.

[13] Larsen C.M., Lie, H., Passano, E., Yttervik, R., Wu, J., Baarholm, G. (2009). VIVANA - Theory Manual, Version 3.7, MARINTEK.

[14] Chaplin, J.R., Bearman, P.W., Cheng, Y., Fontaine, E., Graham, J.M.R., Herfjord, K., HueraHuarte, M., Isherwood, M., Lambrakos, K., Larsen, C.M., Meneghini, J.R., Moe, G., Pattenden, R.J., Triantafyllou, M.S., Willden, R.H.S. (2005). Blind Predictions of Laboratory Measurements of Vortex Induced Vibrations of a Tension Riser. Journal of Fluids and Structures, Vol. 21 (01), pp. 25-40.

[15] Hasselmann, K., Barnett T.P., Bouws E., Carlson D.E., Cartwright D.E., Enke K., Ewing J.A., Gienapp H., Hasselmann D.E., Kruseman P., Meerburg A., Muller P., Olbers D.J., Richter K., Sell W., and Walden H. (1973). Measurements of Wind Wave Growth and Swell Decay during the Joint North Sea Wave Project. (JONSWAP) Deutsches Hydrographische Zeitschrift, Vol 08 (12) PP.1-95.

[16] Ochi, M., K. and Hubble, E., N. (1976). On six-parameters wave Spectra, Proceedings of the 15th Coastal Engineering Conference Vol 1 pp 301-328.

[17] Orcina Ltd, (2003). Orcaflex Version 8.4a7 Manual, Daltongate, Ulverston, Cumbria UK..

[18] Gedikli, E. D, (2014). "Experimental Investigation of Low Mode Number Cylinders Subjected to Vortex Induced Vibrations", M.Sc Thesis, Dept. of Ocean Engineering, University of Rhode Island, USA.

[19] Shi, C., (2011). "Fatigue Damage Prediction in Deepwater Marine Risers due to Vortex-Induced Vibration" PhD Thesis, The University of Texas at Austin, USA.

[20] Chibueze, N.O., Ossia, C.V., Okoli, J.U. (2016). "On the Fatigue of steel catenary risers", Strojniski Vestnik – Journal of Mechanical Engineering, Vol. 62 (12), Pp. 751-756.